Optik 127 (2016) 10322–10334

Contents lists available at ScienceDirect

Optik

journal homepage: www.elsevier.de/ijleo

The research of guidance performance of the phased array seeker with platform for air-to-air missile

Xiao Du*, Qunli Xia

School of Aerospace Engineering, Beijing Institute of Technology, Beijing 100081, People's Republic of China

ARTICLE INFO

Article history:
Received 21 June 2016
Accepted 24 August 2016

Keywords:
Phased array seeker with platform(PASP)
Disturbance rejection effect(DRE)
The parasitic loop
The information for guidance

ABSTRACT

This article aims to meet a hard demand for aircraft about the Disturbance Rejection Effect (DRE) when tracks the target with great maneuver by using the phased array seeker. In order to avoid the severely constraint for seeker, the Phased Array Seeker with Platform(PASP) is put forward firstly. Then the mathematic model of PASP are established. And the feedforward compensation method is used to complete the rate decoupling. By take two methods of platform rate feedforwd into consideration, there are two basic phased array seeker with platform(PASP) seeker structure proposed. Based on that, the transfer function model of the platform phased array seeker of these two structure are established to study the design procedures and performance as well as research. Furth more, the parasitic loop in guidance loop which induced by the PASP DRE is established and the property is analyzed to used for PASP tracking loop and guidance loop design integration. And the research indicated that the PASP has a better performance than any other kinds of seeker in tracking rapidly target and can improve the guidance precision effectively.

1. Introduction

Because of the advantage of large scanning field and outstanding traceability depending on rapidly beam controlling, the phased array seeker (PAS) is suitable for air-to-air missile perfectly, which requires the large field of view and high tracking precision of the seeker when hitting rapid targets. The current researches on PAS mainly focus on strapdown Phased Array Seeker (strapdown PAS), such as the Endo LEAP interception missile project of America air Force [1], "dual range missile" program of the U.S [2], air defense phased array seeker of MBDA company in Europe etc [3–6]. The research results indicate that the influence of disturbance of projectile bodies on the decoupling of line-of-sight rate must be considered when the strapdown PAS is used in the terminal guidance. About decoupling of the line of sight, R. D. Ehrich [7]. has been the first one who proposed to use the feedforward of angular rate of the projectile bodies to realize disturbance decoupling of projectile bodies. Then many scholars have carried out researches on issues existing in the decoupling. Willman et al. have pointed out that the inconformity between beam controlling unit of strapdown PAS and the rate gyroscope will cause the Disturbance Rejection Effect (DRE) of the strapdown seeker [8,9], such as the differentiation of dividing ruler and the dynamics of the two sensors, as well as the quantization of beam control of PAS. Jianmei S et al. analysis the DRE influence to guidance loop and to the seeker performance which induced by senor mismatch [10,11]. Zarchan [12] et al. has studied the influence of parasitic loop of DRE in guidance loop caused by DRE induced by dome slope distort. Wang Jiaxin [13], Fan [14],

* Corresponding author.
E-mail address: duxiao.63@63.com (X. Du).

http://dx.doi.org/10.1016/j.ijleo.2016.08.071

Du Yunli [15], Li Fugui [16], and Song [17] et al. have analyzed the influence of positive feedback of DRE of the strapdown phased array seeker on the stability of guidance loop and precision of terminal guidance. And these results have indicated that the differentiation of dividing ruler between the two sensors is the main reason for the DRE of strapdown PAS, and the influence of the positive feedback of DRE on guidance loop which induce the DRE parasitic loop is more severely. And on the hand, the radar seeker always make its hard to keep the target close to the beam axis to provide accurate measurements [18].

In order to reduce the influence of DRE parasitic loop on missile guidance property, we mostly use calibration on the ground or on-line estimation compensation at present [19,20]. However, to endurance the high precision calibration, different frequency bands and temperatures upon each beam-control code by means of far field calibration method is needed, which will take too much time, which we have analyzed in Ref. [21]. Besides, since the long-term storage the property of the srtapdown PAS can not be ensured, the effect of calibration will surely be weakened, and the expected precision will not be reached. The on-line recognition requires high precision of the model, and the on-line estimation demands sufficient time for estimation, which will greatly restrain the application of phased array seeker in terminal guidance.

The present paper aims to find a solution to decrease the influence of DRE parasitic loop especially for the positive feedback of DRE parasitic loop. Thus a new structure of stable platform applied in the PAS,which is called phased array seeker with platform (PASP), is proposed to reduce the influence of DRE parasitic loop. The structure of the paper is as follows. Firstly the structure of PASP and the angle relationships is presented. And in order to effectively using the space, a structure of rod used in outer gamble and motor driving inter gamble is raised. According to the geometrical relationship of angle, a platform rate feedforwd method is representation. And by taking two methods of acquiring platform rate into consideration, there are two basic PASP controlling scheme proposed. Based on these the transfer function model of the PASP of these two structure are established to studying the design procedure and performance. Secondly, the DRE model and transfer function of these two kinds of structure are established, which demonstrates that the PASP DRE decreases the DRE perfectly and induced a phased lag depended on both platform and phased array radar. Thirdly three kinds of disturbance for PASP are taken into consideration, such as spring moment friction moment and mismatch of beam control coefficient and rate gyroscope coefficient which is called the scale-factor errors. In this part a parasite loop involved by different disturbance, which is called DRE parasitic loop of PASP (PASP DREPL), is analyzed and the different influence to guidance performance is demonstrated. To suitable for the engineering purpose, the DRE of PASP induce by individual disturbance are simplified which in 2 Hz has the same amplitude. Based on the above analysis, the stability region analysis and the effect to equivalent navigation ratio in the time-domain of PASP DRELP system are illustrated, which can useful to design the PASP for tracking a rapidly maneuvering target. And through the researches above, the mathematic model of the phased array seeker with platform is obtained, and the feasibility of the structural concept of phased array seeker with platform is verified, which has laid theoretical basis for the following research.

2. Control system design of phased array seeker with platform

2.1. Operating principle of phased array seeker with platform

The PASP is that phased array antenna is installed on the stabilized platform, which the stabilized platform will isolate the disturbance of missile bodies. In order to use the head space of the projectile bodies to its best, the model of pull rod at the outline border as drive and motor drive in interior casing is adopted, and the schematic diagram is as indicated in Fig. 1.

The relationship between target and missile in three-dimensional is illustrated in Fig. 2a). The cross coupling will not occur by supposing that the rolling moving can be ignored because of stable controlling of rolling channel. And the geometrical relationship of the pitch plane angle of PASP is as indicated in Fig. 2b).

Where x_t is the orientation of target, x_s is beam pointing, x_ϕ refers to normal pointing of interior casing, x_b stands for axial pointing of projectile bodies, ε is the measuring error angle, θ_B is deflection angle between the beam and the plane of antenna, ϕ_y is the angle of the frame of interior casing, ϑ is the attitude angle at the pitching direction of projectile bodies, q_s is the deflection angle between the beam and the inertial space, and q_t refers to the angle of sight of missile target. During the operation of phased array seeker with platform, error angle ε of antenna is obtained through monopulse angle measurement, and at the unit of beam control, the error angle is taken as drive to rotate the beam towards the direction where error angle can be reduce, so as to form field angle θ_B. Then θ_B is taken as the order of the servo system of the platform, and the rotation of the platform will make θ_B as small as possible. When the visual tracking gets stable, the error angle of detector ε, deflection angle of beam θ_B, and the angle of frame of platform, ϕ_y, tends to be stable. And relation indicated in Formula (1) can be obtained

$$\begin{cases} q_t = \vartheta + \phi_y + \theta_B + \varepsilon \\ q_s = \vartheta + \phi_y + \theta_B \end{cases} \tag{1}$$

When the error angle of detector ε gets stable at small value($\varepsilon \approx 0$),$q_t \approx q_s$, and the phased array seeker with platform finishes stable tracking. Then,

$$q_t = \vartheta + \phi_y + \theta_B \tag{2}$$

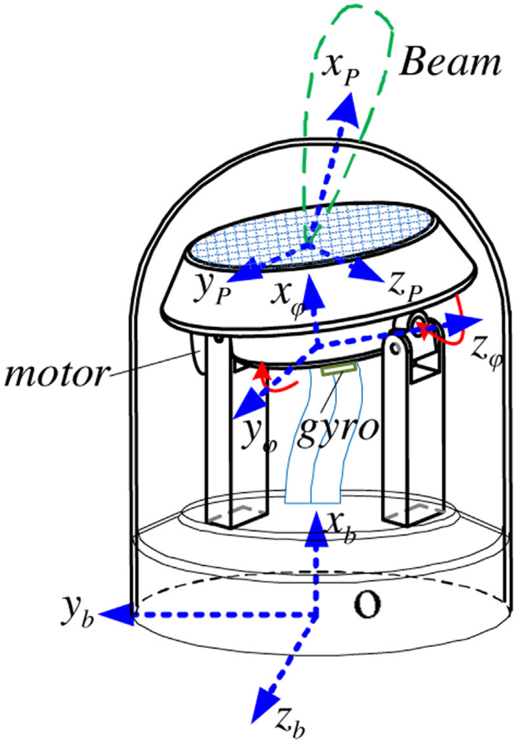

Fig. 1. The structure of phased array seeker with platform (PASP).

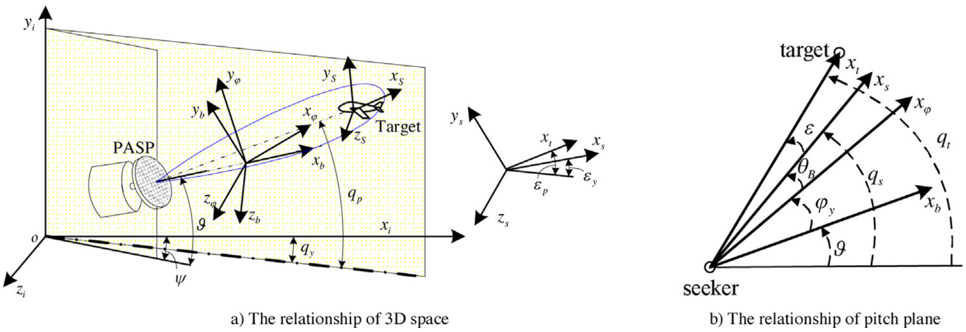

Fig. 2. The angle relationship of PASP.

It can be known through derivation on two sides of Formula (2) that

$$\dot{q}_t = \dot{\vartheta} + \dot{\phi}_y + \dot{\theta}_B \tag{3}$$

where $\dot{\vartheta} + \dot{\phi}_y = \dot{q}_g$ is the measured value of rate gyroscope of the stabilized platform. And Formula (3) can be transformed to Eq. (4).

$$\dot{\theta}_B = \dot{q}_t - \dot{q}_g \tag{4}$$

According to the Eq. (4), the rate of platform should be fed forward to decouple the beam rate. Because of the large bandwidth of stable loop, the rate of platform can be obtained from the command of stable loop or from the rate gyroscope which is strapped on the platform.

2.2. Tracking control system design for PASP

In this paper it is supposed that there is no rolling movement and the PASP system is only discussed for 1-DOF to indicate the basic work theory and control properties. For the stabilized platform, disturbance of friction moment and spring torque

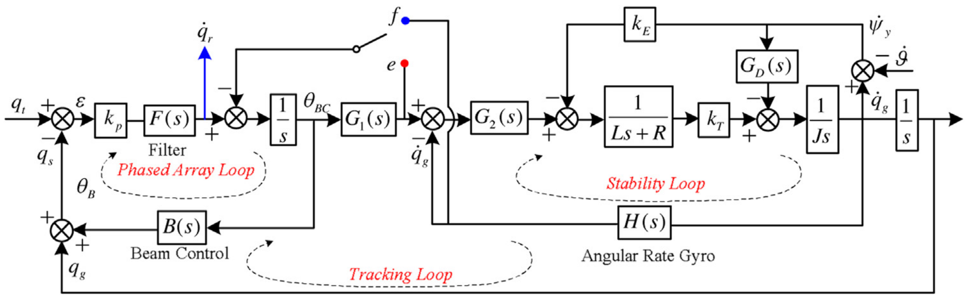

Fig. 3. The Schematic diagram of PASP tracking control system.

caused by pulling of wires exists. The motor dynamic relation of the frame under the influence of disturbance torque can be solved, as indicated in Formula (5).

$$J\ddot{q}_g = T_z - K_v\dot{\phi}_y - K_s\phi_y \tag{5}$$

where J is the rotational inertia of the stabilized platform, T is output torque of servo motor, K_v is damping moment coefficient and K_s is spring torque coefficient. For the convenience of analysis, the disturbance of spring torque and damping moment can be uniformly represented by $G_D(s)$, which expressed as Eq. (6).

$$G_D(s) = K_v + K_s/s \tag{6}$$

According to the statement of 1.1 and Eqs. (2) (4) (5), the schematic diagram of PASP tracking control system is shown in Fig. 3. k_P is the gain of phased array loop and $B(s)$ is transfer function of the beam control unit. $G_1(s)$ and $G_2(s)$ are respectively the regulator and amplifier of the tracking loop and stable loop of the servo control system which is simplified as $G_1(s) = K_1$ and $G_2(s) = K_2$. $H(s)$ is the transfer functions of angular rate gyro. L and R respectively indicate the inductance and capacitance of the servo machine winding, and k_T is moment coefficient of servo motor, k_E is back electromotive force coefficient. $\dot{q}_r$ is the tracking angular rate of the beam relative to inertial space (which can be used for guidance). If not considering the disturbance input of the missile body, then the transfer function of PASP can be expressed as Eq. (7).

$$\begin{aligned} G_{PASP}(s) &= \frac{\dot{q}_r}{\dot{q}_t}(s) \\ &= \frac{k_P\left\{s\left[Js(Ls+R) + k_T G_2(s)H(s)\right] + k_T G_1(s)G_2(s)H(s)\right\}}{s\left\{s\left[Js(Ls+R) + k_T G_2(s)H(s)\right] + k_T G_1(s)G_2(s)H(s)\right\} + k_P\left\{s\times B(s)\left[Js(Ls+R) + k_T G_2(s)H(s)\right] + k_T G_1(s)G_2(s)\right\}} \end{aligned} \tag{7}$$

Suppose the phased array beam control unit $B(s)$ is perfect and the bandwidth of rate gyro $H(s)$ is wide enough to approximate as $B(s) \approx H(s) \approx 1$. Then Formula (7) is transformed into Formula (8).

$$G_{PASP}(s) = \frac{\dot{q}_r}{\dot{q}_t}(s) = \frac{k_P}{s+k_P} = \frac{1}{T_{PASP}s+1} \tag{8}$$

where $T_{PASP} = 1/k_P$. Thus the tracking rate of PASP is all depend on the beam control unit. That is to say, when the beam control unit realizes ideal control, and the transfer ratio of rate gyroscope is 1, the characteristics of the tracking object of PASP is the same to strapdown PAS.

2.3. Example

According to the last section,the PASP has the most outstanding performance of tracking rapid target. And the typical parameter of PASP is shown in Table 1.

In order to verify the tracking performance, the simulation of tracking zenith pass target and step target is analyzed. The relative position of zenith pass is shown in Fig. 4. The vertical distance between PASP and target is 120m, and the horizontal distance between PASP and target is 1000m. The results is illustrated in Figs. 5 and 6.

The simulation result of tracking step target is shown in Figs. 7 and 8.

Based on these analysis, the PASP can track the rapid target perfectly according to Figs. 6 and 8. According to Figs. 5 and 7, during the tracking process, the target can keep in the beam because of the error angle is less than 2°. And because of the stabilized platform, the beam angle can keep a little angle which can reduce the beam control error.

Table 1
The parameter of PASP.

Parameter	Value
Rotational inertia	$J = 0.002099$ kg m
Moment coefficient	$k_{T = 0.2344\,\mathrm{Nm/A}}$
Inductance	L = 0.0035H
Resistance	R = 8Ω
Back electromotive force coefficient	$k_{E = 0.2344\,\mathrm{V/rad/s}}$
Gain of tracking loop	$G_1(s) = 12$
Gain on stabile loop	$G_2(s) = 12$
Angular rate gyro	$H(s) = 1/\left(0.0000004s^2 + 0.0028s + 1\right)$
Gain of phased array loop	$k_P = 126$
Beam controlling unit	$B(s) = 1 + \Delta B(\lvert\Delta B\rvert \le 0.05$ after calibration)
Filter	$F(s) = 1$

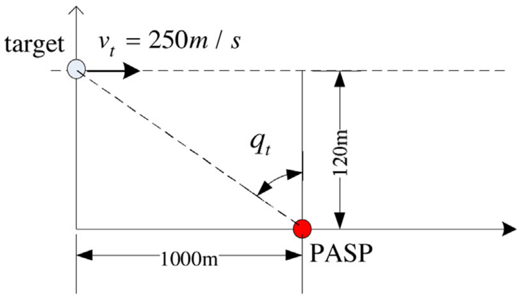

Fig. 4. The relative position for zenith pass.

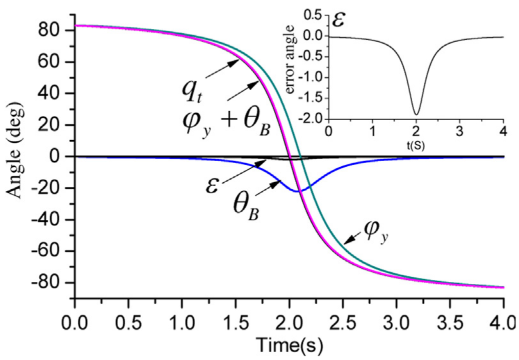

Fig. 5. The angle of PASP (zenith pass).

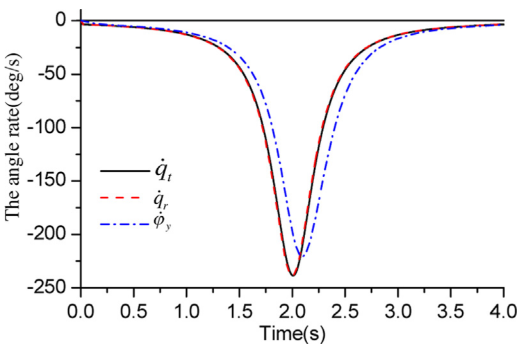

Fig. 6. The angle rate of PASP (zenith pass).

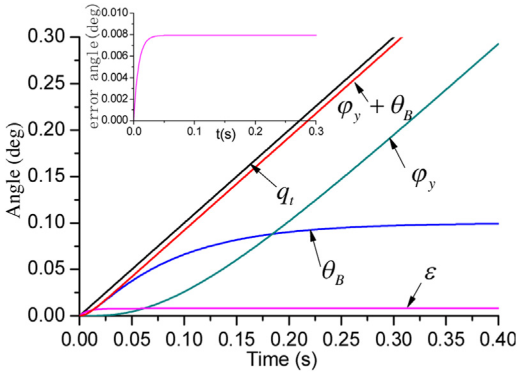

Fig. 7. The angle of PASP (step).

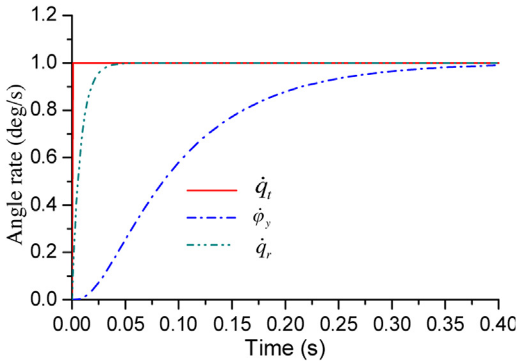

Fig. 8. The angle rate of PASP (step).

3. The mathematic model of the DRE

3.1. Establishment of DRE model

The DRE stand for the capacity of isolating the disturbance of projectile bodies. The smaller the DRE magnitude is, the stronger the isolation of seeker against the disturbance will be. Suppose the angular velocity of missile attitude is $\dot{\vartheta}(t)$, and the decoupling error of seeker on the angular velocity of the line of sight is $\Delta\dot{q}(t)$, and thus the DRE can be defined as Eq. (9).

$$R(t) = \Delta\dot{q}(t)/\dot{\vartheta}(t) \tag{9}$$

Carry out Laplace transformation, and then the transfer function of isolation can be presented as,

$$R(s) = \Delta\dot{q}(s)/\dot{\vartheta}(s) \tag{10}$$

Fig. 9 can be obtained through equivalent transformation of the system principle diagram of PASP indicated in Fig. 3.

According to Fig. 9, the phased array seeker with platform contains two parts, phased array loop and platform loop, and the equivalent diagram is as indicated in Fig. 10where $G_{PS}(s)$ stands for the dynamic transfer function of the platform, and $R_{PS}(s)$ stands for the transfer function of DRE of platform. $R_{PAS}(s)$ stands for transfer function of DRE of phased array. It can be known from the equivalent PASP model of pitch plane that the disturbance of attitude angular rate of projectile body is coupled into the angular rate of platform $\dot{\psi}_y$ through friction moment and damping moment of the stabilized platform, and then coupled into the beam control loop of phased-array antenna through angular rate gyro of the stabilized platform, at last to influence the output signal $\dot{q}_r$. Hence, the disturbance of attitude angular rate of projectile body will pass through two-grade transfer. Then, the transfer function from body angular rate to angular rate of the line of sight can be expressed as:

$$R_{PASP}(s) = \frac{R_{PS}(s) \times R_{PAS}(s)}{1 - G_{PS}(s) \times R_{PAS}(s)} \tag{11}$$

It can be known through Equality(11) that the denominator $1 - G_{PS}(s) \times R_{PAS}(s)$ of the transfer function of isolation of PASP which includes the dynamic transfer function of the platform $G_{PS}(s)$ and transfer function of isolation of phased array

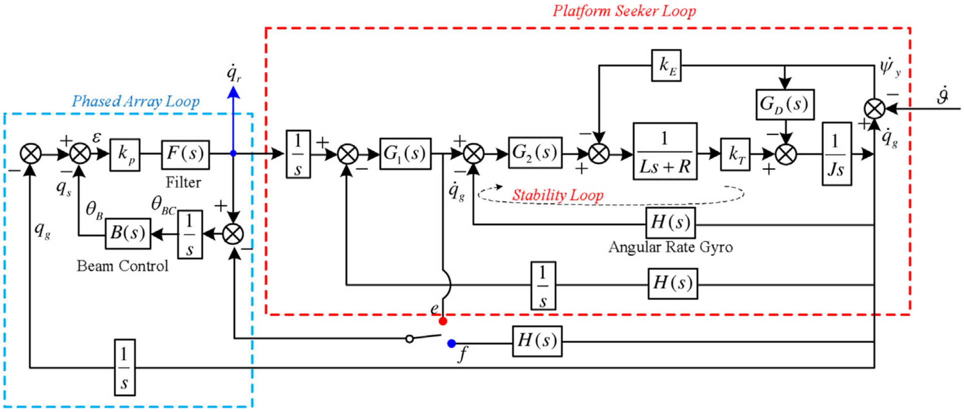

Fig. 9. The equivalent diagram of PASP tracking control system.

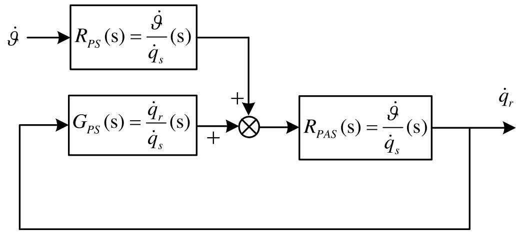

Fig. 10. The equivalent function diagram of PASP.

$R_{PAS}(s)$. According to Fig. 5, the transfer function of platform with different signal getting points (e and f) is as shown in Formulas (12) and (13). And the DRE function of different point (*e* and *f*) are shown in Formulas (14) and (15).

$$G_{PS}^{f}(s)=\frac{\dot{q}_g}{\dot{q}_t}(s)=\frac{H(s)}{\frac{J(Ls+R)}{G_1(s)G_2(s)k_T}s^2+\frac{[G_D(s)(Ls+R)+k_Ek_T+G_2(s)k_TH(s)]}{G_1(s)G_2(s)k_T}s+1} \tag{12}$$

$$G_{PS}^{e}(s)=\frac{\dot{q}_g}{\dot{q}_t}(s)=\frac{\frac{(Ls+R)Js+G_D(s)(Ls+R)+k_Ek_T}{G_2(s)k_T}+H(s)}{\frac{J(Ls+R)}{G_1(s)G_2(s)k_T}s^2+\frac{[G_D(s)(Ls+R)+k_Ek_T+G_2(s)k_TH(s)]}{G_1(s)G_2(s)k_T}s+1} \tag{13}$$

$$R(s)_{PS}^{f}=\frac{H(s)\left(\frac{k_Ek_T+G_D(s)(Ls+R)}{G_2(s)k_T}\right)\times\frac{s}{G_1(s)}}{\frac{J(Ls+R)}{G_1(s)G_2(s)k_T}s^2+\frac{[G_D(s)(Ls+R)+k_Ek_T+G_2(s)k_TH(s)]}{G_1(s)G_2(s)k_T}s+1} \tag{14}$$

$$R(s)_{PS}^{e}=\frac{-\frac{k_Ek_T+G_D(s)(Ls+R)}{G_2(s)k_T}}{\frac{J(Ls+R)}{G_1(s)G_2(s)k_T}s^2+\frac{[G_D(s)(Ls+R)+k_Ek_T+G_2(s)k_TH(s)]}{G_1(s)G_2(s)k_T}s+1} \tag{15}$$

Since the rotational inertia of the platform J is small, inductance L and resistance R of the servo motor can be ignored when compared to the ride gain $G_1(s)G_2(s)$. Then Formulas (12) (13) (14) and (15) can be transformed into formula below.

$$G_{PS}^{f}(s)\approx G_{PS}^{e}(s)=\frac{\dot{q}_g}{\dot{q}_t}(s)=\frac{H(s)}{T_{PS}s+1} \tag{16}$$

$$R(s)_{PS}^{f}=\frac{K_{PS\_R}}{T_{PS}s+1}\times\frac{s}{G_1(s)} \tag{17}$$

$$R(s)_{PS}^{e}=-\frac{K_{PS\_R}}{T_{PS}s+1} \tag{18}$$

Where the dynamic time constant of seeker with platform is: $T_{PS}=[G_D(s)(Ls+R)+k_Ek_T+G_2(s)k_TH(s)]/G_1(s)G_2(s)k_T$ Because the $G_D(s)$ and k_Ek_T can be omitted compared with $G_1(s)G_2(s)k_T$, and $(Ls+R)\approx 1$, thus the time constant can be simplified as Formula (19).

$$T_{PS}=1/G_1(s) \tag{19}$$

And the DRE function of phased array loop is:

$$R(s)_{PAS} = \frac{K_{PAS\_R}}{T_{PAS}s + 1} \tag{20}$$

where $T_{PAS} = 1/k_P B(s)$ is the time constant of phased array loop, $K_{PAS\_R} = \Delta B$ is gain of DRE of phased array loop. According to the Eq. (20), the DRE of Phased array loop is always induced by the scale inconformity between the beam control unit and the rate gyro. And K_{PAS_R} can be limited to $-0.05 \sim 0.05$ because of the $H(s)$ and $1/B(s)$ are both approximate to 1.

$$G_{inner}(s) = \frac{R_{PAS}(s)}{1 - G_{PS}(s) \times R_{PAS}(s)} = \frac{K_{PAS\_R}}{T_{PAS}s + 1} / (1 - \frac{1}{T_{PS}s + 1} \times \frac{K_{PAS\_R}}{T_{PAS}s + 1}) \tag{21}$$

Suppose the ratio of time constant of tracking loop of phased array to the dynamic time constant of stabilized platform is α ($T_{PAS} = \alpha T_{PS}$), and Formula (21) can be converted into Formula (22).

$$G_{inner}(s) = \frac{(T_{PS}s + 1)K_{PAS\_R}}{\alpha T_{PS}^2 s^2 + (\alpha + 1)T_{PS}s + 1 - H(s)K_{PAS\_R}} \tag{22}$$

According to Routh stability criterion,

$$H(s)K_{PAS\_R} < 1 \tag{23}$$

Since $H(s)$ is the transfer function of rate gyroscope, and its value approximates 1. According to Formula (20) the K_{PAS_R} can be limited to $-0.05 \sim 0.05$, thus the value of $H(s)$ and K_{PAS_R} can ensure the validity of Formula (23). And it can be known through Formula (23) that the stability of loop within isolation will not affected by the ratio α. It can be concluded through characteristic analysis on Formula (20) that $R_{PAS}(s)$ is a small element close to 0, and $G_{PS}(s)$ is approximate to 1 and less 1, so $1 - G_{PS}(s) \times R_{PAS}(s) \approx 1$; the $G_{inner}(s)$ can be expressed as,

$$G_{inner}(s) \approx R_{PAS}(s) \tag{24}$$

In the subsequent analysis in this article, the loop within isolation of phased array seeker can be ignored, so as to get the simplified transfer function of isolation of phased array seeker with platform.

$$R^f_{PASP}(s) \approx R^f_{PS}(s) \times R_{PAS}(s) = \frac{s}{G_1(s)} \times \frac{K_{PS\_R}}{T_{PS}s + 1} \times \frac{K_{PAS\_R}}{T_{PAS}s + 1} \tag{25}$$

$$R^e_{PASP}(s) \approx R^e_{PS}(s) \times R_{PAS}(s) = -\frac{K_{PS\_R}}{T_{PS}s + 1} \times \frac{K_{PAS\_R}}{T_{PAS}s + 1} \tag{26}$$

It can be concluded that the DRE of PASP is determined by multiplying the DRE of stable platform and that of the phased array loop, so as to greatly reduce amplitude of DRE to improve the property of PASP. When the capacity of platform to resisting disturbance is good enough, namely, very small amplitude of DRE, the outstanding isolation characteristic can be realized to avoid the influence of disturbance of projectile bodies on quality of guidance signal. Take the different disturbance torque in to consideration, the DRE gain of stable platform can be expressed as Eq. (27) and can be expressed individualized according to Eq. (6) as Eq. (28).

$$K_{PS\_R} = [k_E k_T + G_D(s)(Ls + R)] / G_2(s) k_T \tag{27}$$

$$\begin{cases} K_{PS\_R} = k_E / G_2(s) & (G_D(s) = 0, (Ls + R) = 1) \\ K_{PS\_R} = K_v / G_2(s) k_T & (G_D(s) = K_v, k_E = 0, (Ls + R) = 1) \\ K_{PS\_R} = K_s / s G_2(s) k_T & (G_D(s) = K_s / s, k_E = 0, (Ls + R) = 1) \end{cases} \tag{28}$$

From the Eq. (28), the DRE of platform is induced by the back-EMF (electromotive force), damping torque and spring torque. The gain is in direct proportion to the parameter of $k_E K_v$and K_s, and is inversely proportional to the $G_2(s)$, that is the larger bandwidth of inner loop the smaller of DRE magnitude is. Because of the $k_E k_T \approx 0$, the DRE induced by the back-EMF can be omitted. According to the Eqs. (26) and (8), the time constant can be expressed as $T_{PASP\_R} = (1 + \alpha)T_{PASP}$, the α stands for the ratio of phased array loop time constant and stable platform time constant. Because of $1 \ll \alpha$, the time constant can be expressed as $T_{PASP\_R} = \alpha T_{PASP}$. Convenient for analysis the $G_1(s) = K_1$ and $G_2(s) = K_2$, and the Eqs. (25) and (26) can be simplified to Eqs. (29) and (30).

$$R^f_{PASP}(s) \approx \frac{s}{K_1} \frac{K_{PS\_R} \times K_{PAS\_R}}{(1 + \alpha)T_{PASP}s + 1} = \frac{(K_v s + K_s) K_{PAS\_R}}{K_1 K_2 k_T [(1 + \alpha)T_{PASP}s + 1]} = \frac{(K_v s + K_s) K_R}{K_1 [(1 + \alpha)T_{PASP}s + 1]} \tag{29}$$

$$R^e_{PASP}(s) \approx -\frac{K_{PS\_R} K_{PAS\_R}}{(1 + \alpha)T_{PASP}s + 1} = -\frac{(K_v s + K_s) K_{PAS\_R}}{K_2 k_T [(1 + \alpha)T_{PASP}s + 1] s} = -\frac{(K_v s + K_s) K_R}{[(1 + \alpha)T_{PASP}s + 1] s} \tag{30}$$

where $K_R = K_{PAS\_R}/K_2 k_T$.The ration of DRE transfer function based on different signal pick up points (e and f) can be expressed as Eq. (31), which according to the Eqs (29) and (30).

$$R^e_{PASP}/R^f_{PASP} = -K_1/s \tag{31}$$

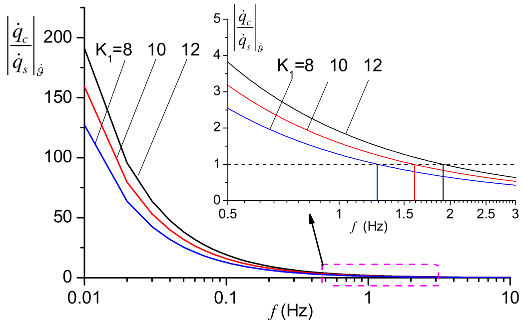

Fig. 11. The magnitude relation of different feedforward points.

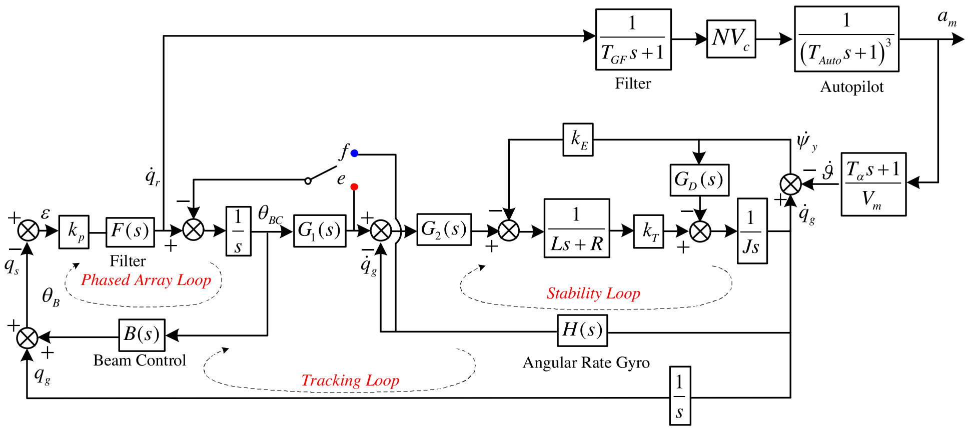

Fig. 12. The Guidance Parasitic Loop.

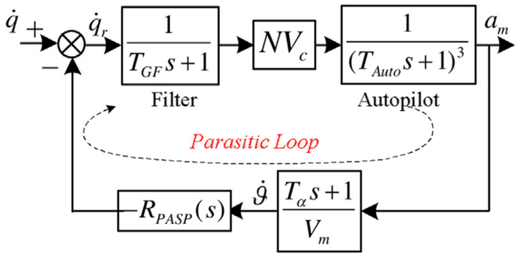

Fig. 13. Simplified model the PASP guided missile system.

The relation of DRE with different feedforward point is shown in Fig. 11.

According to Fig. 11, despite the disturbance torque, the ratio of transfer function of DRE with different feedforward point is K_1/ω, which is in direct proportion to the K_1 and is inversely proportional to ω. And when the $f = K_1$, the magnitude of DRE is the same. Thus in the usually working frequency of air missile (2 Hz), when $K_1 = 10$, the DRE of $R^f_{PASP}(s)$ is equal to $R^e_{PASP}(s)$. But the sign is decided by both the guidance point and the phased array loop gain. When the point is e and the $K_R < 0$, the DRE of PASP is positive, otherwise the $K_R > 0$, the DRE of PASP is negative. When the point is f and the $K_R > 0$, the DRE of PASP is positive, otherwise the $K_R < 0$.

4. The stability region analysis of PASP system

4.1. The model of DRE parasitic loop

In terminal guidance phase, the PASP provide the guidance signal, the schematic diagram is shown in Fig. 12. In this phased if the seeker provide the guidance signal which can not isolation the body disturbance perfectly, the guidance signal with body motion will influence the missile attitude information, and hence the parasitic loop is stimulated, which is called the DRE parasitic loop (DREPL). The simplified DREPL is shown in Fig. 13.

Table 2
DRE model of 2 Hz.

Feed forward point	Equivalent Gain	Transfer function
f	$K_s K_R/K_1 = 1.55R_{2Hz}$	$R_{f\_s}(s) = \frac{1.55\times R_{2Hz}}{T_{PASP\_R}s+1}$
	$K_v K_R/K_1 = 0.13R_{2Hz}$	$R_{f\_v}(s) = \frac{0.13\times R_{2Hz}s}{(T_{PASP\_R}s+1)}$
e	$K_s K_R = 19.5R_{2Hz}$	$R_{e\_s}(s) = -\frac{19.5\times R_{2Hz}}{(T_{PASP\_R}s+1)s}$
	$K_v K_R = 1.6R_{2Hz}$	$R_{e\_v}(s) = -\frac{1.6\times R_{2Hz}}{T_{PASP\_R}s+1}$

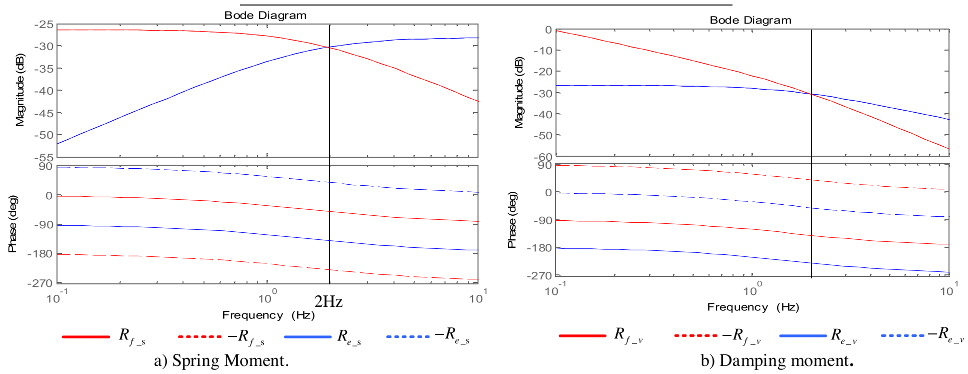

Fig. 14. Bode of DRE with 2 Hz equation.

Because of the DREPL, the dynamic characteristic of guidance loop would become worse, which may induce the instability of guidance loop. In order to analyze the stability of DREPL, the guidance filter can be simplified as $G_{GF}(s) = 1/(T_{GF}s + 1)$, the time constant of guidance filter is $T_{GF} = T_{PASP\_R}$. The autopilot can be expressed as $G_{aut}(s) = 1/(T_{Auto}s + 1)^3$, and the time constant of autopilot is $T_{Auto} = T_{PASP\_R}$,that is the time constant of autopilot is three time as PASP. The T_α is aerodynamics turning rate time constant (ATRTC). $K_x = NV_c/V_m$ is a combined parameter which stand for the relation of missile and target. And according to the last section, the guidance signal have the different characteristics base on the different feed forward point. Then make the different DRE function have a same amplitude in 2 Hz, the DRE function can be expressed in a uniform style in the Table 2.

When $T_{PASP\_R} = 0.1s$ and $R_{2Hz} = \pm 0.03$, the bode figure is shown in Fig. 14. The a) is the DRE of Spring moment. And the b) is the DRE of damping moment. The blue line stand for the DRE which feed forward signal pick up from point e. And the red line stand for the DRE which feed forward signal pick up from point *f*. By analysing the magnitude-frequency characteric of these DRE, in the low frequency, the DRE magnitude which feed forward from point *e* is smaller than the DRE magnitude which feed forward from point *f*. On the contrary, in the high frequency the DRE magnitude which feed forward from point *e* is bigger than the DRE magnitude which feed forward from point *f*. In the phase-frequency characteristic, the dash line stand for the phased array scale factor is negative, and the solid line stand for the phased array scale factor is positive.

In order to analysis the influence to the DREPL which induced by different DREs, the open loop function of DREPL can be expressed as Eq. (31).

$$G_{DREPL}(s) = \frac{N\frac{V_c}{V_m}(T_\alpha s + 1)}{(T_{PASP\_R}s + 1)^4} R_{PASP}(s) \tag{31}$$

AccordingtoEq.31, theopenlooptransferfunctionofPASPcanbeexpressasEq.(32)

$$\phi\left(\frac{\omega}{\omega_{PASP\_R}}\right) = \phi_x - 5 \times \arctan\left(\frac{\omega}{5\omega_{PASP\_R}}\right) + \arctan\left(\frac{T_\alpha}{T_{PASP\_R}} \frac{\omega}{\omega_{PASP\_R}}\right) \tag{32}$$

The ϕ_x is the phased lag of different model of PASP.

I. When $K_R > 0$ and $R_{PASP} = R_{f\_s}$, the $\phi_x = -180^\circ$; When $R_{PASP} = R_{e\_s}$ the $\phi_x = -90^\circ$; When $R_{PASP} = R_{f\_v}$ the $\phi_x = -90^\circ$; When $R_{PASP} = R_{e\_v}$ the $\phi_x = 0^\circ$

II. When $K_R < 0$ and $R_{PASP} = R_{f\_s}$ the $\phi_x = 0^\circ$; When $R_{PASP} = R_{e\_s}$ the $\phi_x = -270^\circ$; When $R_{PASP} = R_{f\_v}$ the $\phi_x = 90^\circ$; When $R_{PASP} = R_{e\_v}$ the $\phi_x = -180^\circ$. Thus the stable frequency interval of different DRE model is shown in Fig. 15.

The Fig. 15 demonstrates the unstable frequency boundary of different DRE models. The x axis is stand for the ratio of T_α (ATRTC) and the time constant of PASP DRE. According to Fig. 15, no matter in the left plane or in the right plane, the unstable frequency will increase to a constant. In the right plane the parameter K_R is positive and in the left plane the parameter is negative. When K_R is negative that the phased array graduated scale is negative, the unstable frequency boundary of DRE model which use the gyro signal to feedforward. In the left plane the unstable frequency boundary of different DRE models

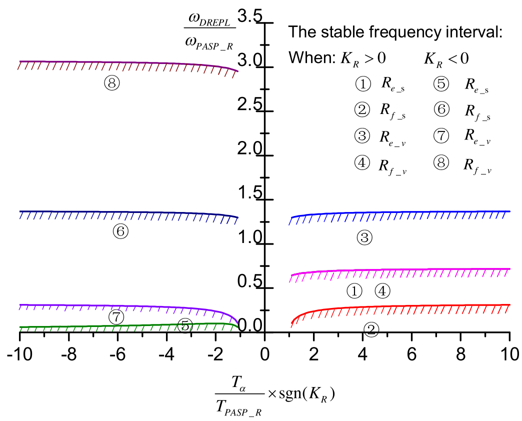

Fig. 15. The stable frequency interval of different DRE model.

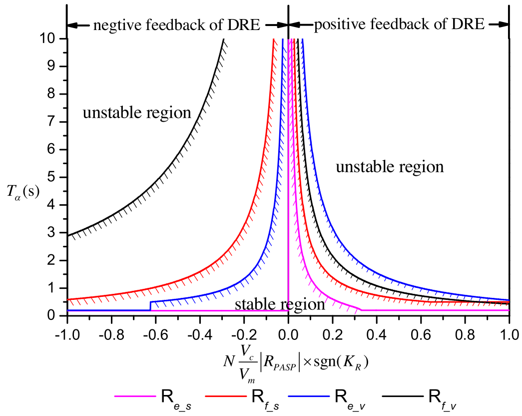

Fig. 16. The stable region on PASP.

in sequence are R_{f_v} R_{f_s} R_{e_v} and R_{e_s}. In the right plane the unstable frequency boundary of R_{e_v} is the highest, which is 1.32 times than the bandwidth of PASP. Then the unstable frequency boundary of R_{e_s} and R_{f_v}. And the last is R_{f_s}. Because of the most common frequency of missile guidance signal is lower than the seeker bandwidth, the unstable frequency of PSAPLP should as higher as possible. Furthermore the stable area is both depend on not only the phase but also the amplitude. Thus the Routh stability criterion is used. Then the closed DREPL function can be expressed as Eq. (33):

$$G_{paralitic}(s) = \frac{G_{GF}(s)G_{aut}(s)NV_c}{1 - K_x(T_a s + 1)G_{GF}(s)G_{aut}(s)R_{PASP}(s)} \tag{33}$$

According to Fig. 8, the sign have a lage influence on the phase-frequency characteristic of APAS. Then it will influence the stability of DREPL. When the $R_{PASP}(s)$ in Fig. 8 is replaced with the transfer function in Table 1, as will as according to Routh stability criterion, the stable region can be illustrate in Fig. 11.

The Fig. 16 illustrate the stable region of DREPL induced by string torque and damping torque with different feed forward point. From Fig. 16, when the R_{f_v} is negative, the area of stable region is largest; and when R_{e_s} is negative, the area of stable region is smallest (the DREPL system can not keep stable). By sum the region, the R_{f_v} that DRELP induce by damping torque and feed forward from f point is the biggest; the stable region of R_{f_s} and R_{e_v} is equal mainly; the stable region of R_{e_s} is smallest. Above all, in view of the DREPL it is reasonable to get the feed forward signal for phased array loop from the rate gyro (f point).

4.2. The time domain property of DREPL induced by PASP DRE

The DRELP not only influence the stability of guidance loop but also effect the navigation ratio which will influence the ability of eliminate error which reflect the time domain feature. In order to analysis the time domain characteristic, we can get the transfer function from the acceleration to guidance signal when s tend to zero. The different equation is illustrate below.

Table 3
The ratio of $\omega_{DREPL}/\omega_{PASP\_R}$.

$sgn(K_R)$	R_{e_s}	R_{f_s}	R_{e_v}	R_{f_v}
−1	0.1	1.32	0.3	3
1	0.66	0.3	1.32	0.66

Table 4
The parameter of typical scenario.

T_{PASP_R}(s)	T_{α}(s)	V_c (m/s)	V_m (m/s)	R_{PAS}	R_{PS}	K_R
0.1	1.5	450	300	0.05	0.4	±0.2

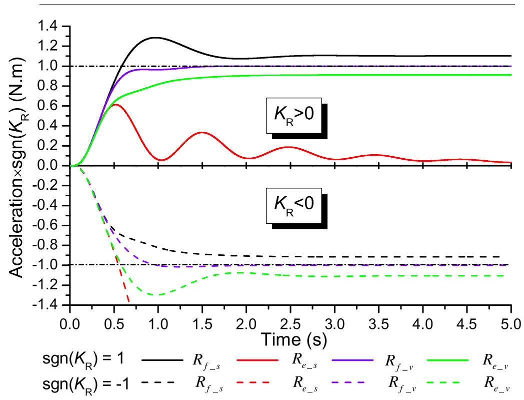

Fig. 17. The time domain of DREPL.

a) The equivalent navigation ratio which influenced by DREPL induced by spring torque

The Eq. (34) is about the feed forward signal for phased array loop from point *e*. And the Eq. (35) is about the feed forward signal for phased array loop from point *f*.

$$N_{EF} \underset{s\to 0}{=} \frac{a_m}{\dot{q}_t}\Big|_s^e = \frac{(T_{PASP\_R}s+1)sNV_c}{(T_{PASP\_R}s+1)^5 s \pm 19.5R_{2\mathrm{Hz}}N\frac{V_c}{V_m}(T_\alpha s+1)}\Big|_{s\to 0} = 0 \tag{34}$$

$$N_{EF} \underset{s\to 0}{=} \frac{a_m}{\dot{q}_t}\Big|_s^f = \frac{(T_{PASP\_R}s+1)NV_c}{(T_{PASP\_R}s+1)^5 \pm 1.55R_{2\mathrm{Hz}}N\frac{V_c}{V_m}(T_\alpha s+1)} \underset{s\to 0}{=} \frac{NV_c}{1 \pm 1.55R_{2\mathrm{Hz}}N\frac{V_c}{V_m}} \tag{35}$$

b) The equivalent navigation ratio which influenced by DREPL induced by damping torque

The Eq. (36) is about the feed forward signal for phased array loop from point *e*. And the Eq. (37) is about the feed forward signal for phased array loop from point *f*.

$$N_{EF} \underset{s\to 0}{=} \frac{a_m}{\dot{q}_t}\Big|_v^e = \frac{(T_{PASP\_R}s+1)NV_c}{(T_{PASP\_R}s+1)^5 \pm 1.6R_{2\mathrm{Hz}}N\frac{V_c}{V_m}(T_\alpha s+1)} \underset{s\to 0}{=} \frac{NV_c}{1 \pm 1.6R_{2\mathrm{Hz}}N\frac{V_c}{V_m}} \tag{36}$$

$$N_{EF} \underset{s\to 0}{=} \frac{a_m}{\dot{q}_t}\Big|_v^f = \frac{(T_{PASP\_R}s+1)NV_c}{(T_{PASP\_R}s+1)^5 \pm 0.13\times R_{2\mathrm{Hz}}N\frac{V_c}{V_m}(T_\alpha s+1)s} \underset{s\to 0}{=} NV_c \tag{37}$$

According to the derivation above, the DRE induced by damping torque has little influence on equivalent navigation ratio, but influence of the DRE induced by spring torque is bigger, especially when the feed forward signal for phased array loop is picked up from the command of stable platform (*e* point), the equivalent navigation ratio will became zero.

4.3. Example

Then a set of parameter of typical scenario is list in Tables 3 and 4.

With the typical parameter established in Table 4, the time domain result is shown in Fig. 17. The y axis is stand for the missile acceleration according to the proportional navigation multiply with sign function $\mathrm{sgn}(K_R)$. The positive side is stand for the $K_R > 0$, and the negative is stand for the $K_R < 0$. Both in the negative and positive the R_{e_s} make the acceleration worst. Thu in the view of time domain, the feed forward signal for phased array should be pick up from the rate gyro to reduce the influence to the equivalent navigation ratio. But take noise into consideration in the engineering, the signal from rate gyro will disturbance by noise severely, which is the following research for this task.

5. Conclusion

Through the researches above, the mathematic model of the phased array seeker with platform is obtained, and the feasibility of the structural concept of phased array seeker with platform is verified, which has laid theoretical basis for the following research.

Based on these analysis, the PASP not only can track the rapid target as quickly as phased array seeker but also can keep the target in the beam with an error angle less than 2°. And because of the stabilized platform, the beam angle can keep a little angle which can reduce the beam control error. Thus the beam calibration can be used in a small rang such as $\pm 30^{\circ}$ which save a large time used to calibration.

And based on analysis the characteristic of DRE of PASP and tracking ability of PASP, the tracking ability is rely on the phased array loop and the DRE is rely on both the phased array and the stable platform which magnitude is the multiplication of DRE of phase array loop and stable platform and phase is sum of them. Thus the tracking bandwidth of platform can be decreased and the error of phased array scale factor can also be bigger on some level. So it can reduce the workload of phased array radar calibration. By comparing the different method of picking up feed forward signal for phased array loop, and take the frequency and time characteristic of PASP to consideration, it is reasonable to pick up from the rate gyro. But a suitable filter should be designed to reduce the noise.

References

[1] R.S. Webb, S.R. Carpenter, Design of A W-Band Active Phased Array for Missile Interceptor Seekers, AIAA93-2645.
[2] Luigi Proietti, Cecchini-Emidio Pizzingrilli, Simone Russ-Ugo, F. D'Elia, MMW Active Phased Array Seeker Project for Hit to Kill Engagement, IEEE 1-4244-1539-X/08, (2008).
[3] B. Schwerdt Chris, Noman F. Powell, ect., Some Technology Innovations in MMW Seeker for Endoatmospheric Interceptors, AIAA93-2650.
[4] L.P. Cecchini, E. Pizzingrilli, S. Russo, et al., MMW active phased array seeker project for Hit To Kill engagement//*Radar Conference*, (2008). RADAR'08. IEEE. IEEE, 2008: 1–6.
[5] A.J. Fenn, D.H. Temme, W.P. Delaney, et al., The development of phased-array radar technology, Lincoln Lab. J. 12 (2) (2000) 321–340.
[6] C.R. Janice, H.M. James, P.B. Joel, et al., The past, present, and future of electronically-steerable phased arrays in defense application, Proceedings of Aerospace Conference, IEEE, 2008: 1–7.
[7] R.D. Ehrich, P. Vergez, Strapdown Seeker Technology for the Terminal Guidance of Tactical Weapons, ADA092606, (1980).
[8] Warren W. Willman, Effects of strapdown seeker scale-factor uncertainty on optimal guidance, J. Guidance Control Dyn. 11 (3) (1988) 199–206.
[9] Se-Ah Jang, Guidance Algorithms for tactical missile with strapdown seeker, SICE Annual Conference, (2008) 2616–2619.
[10] S. Jianmei, C. Gaohua, C. Xianxiang, et al., Stability region analysis of the parasitic loop of the semi-strapdown homing seeker, Proc. Inst. Mech. Eng. I: J. Syst. Control Eng. 226 (4) (2012) 550–562.
[11] J. Song, G. Cai, L. Kong, et al., The guidance system design of the semi-strapdown homing guided missile, Proc. Inst. Mech. Eng. I: J. Syst. Control Eng. 226 (6) (2012) 761–774.
[12] F.W. Nesline, P. Zarchan, Radome induced miss distance in aerodynamically controlled homing missiles AIAA84-1824, [S.L.]: AIAA, (1984) 99–115.
[13] Jia-xin Wang, De-fu Lin, Zai-kang Qi, et al., Study on disturbance rejection rate parasitical loop of strapdown phased array radar seeker, Trans. Beijing Inst. Technol. 33 (11) (2013) 1124–1129.
[14] Huitao Fan, Jun Yang, Xueping Zhu, Research on beam stable technology of phased array radar seeker, Acta Aeronaut. et Astronaut. Sin. 34 (2) (2013) 387–392.
[15] Yunli Du, Qunli Xia, Zaikang Qi, Research on effect of seeker disturbance rejection rate with phase lag on stability of parasitical loop, Acta Armamentarii 32 (1) (2011) 28–32.
[16] Fugui Li, Qunli Xia, Zaikang Qi, Effect of parasitic loop on strap-down seeker and compensated with identification method, Syst. Eng. Electron. 35 (8) (2013) 1717–1722.
[17] Tao Song, Defu Lin, Jiang Wang, Influence of seeker disturbance rejection rate on missile guidance system, J. Harbin Eng. Univ. 34 (10) (2013) 1234–1241.
[18] V. Saini, Air-to-air tracking of a maneuvering target with gimbaled radar, J. Guidance Control Dyn. (2015) 1–13.
[19] Li Hong, Xue Bing, Yang Ying-ke, et al., The technology of measuring and testing phased array antennas, China Meas. Technol. 5 (2003) 10–14.
[20] Paul Zarchan, Harvey Gratt, Adaptive radome compensation using dither, AIAA96-3879, San Diego, (1996).
[21] D. Xiao, X. Qunli, et al., The calibration method of phased array seeker with the phantom-bit technology, Int. J. Light Electron Opt. (2016), http://dx.doi.org/10.1016/j.ijleo.2016.05.066.